Proc. Natl. Acad. Sci. USA
Vol. 96, pp. 1657–1662, February 1999
Neurobiology

Localization of Niemann–Pick C1 protein in astrocytes: Implications for neuronal degeneration in Niemann–Pick type C disease

SHUTISH C. PATEL*†, SUNDAR SURESH*, UJENDRA KUMAR‡, C. Y. HU§, ADELE COONEY¶, E. JOAN BLANCHETTE-MACKIE‖, EDWARD B. NEUFELD‖, RAMESH C. PATEL**, ROSCOE O. BRADY¶, YOGESH C. PATEL‡, PETER G. PENTCHEV¶, AND WEI-YI ONG§

*Neurobiology Research Laboratory, Veterans Affairs Connecticut Healthcare System, Newington, CT 06111; ‡Fraser Laboratories, McGill University, Montreal, Canada H3A1 A1; ¶Section of Cellular and Molecular Pathophysiology, Building 10, Room 3D-12, Developmental and Metabolic Neurology Branch, National Institute of Neurological Disorders and Stroke, National Institutes of Health, Bethesda, MD 20892; ‖Section of Lipid Cell Biology, National Institute of Neurological Disorders and Stroke, Building 8, Room 427, National Institutes of Health, Bethesda, MD 20892; **Department of Chemistry, Clarkson University, Potsdam, NY 13676; and §Department of Anatomy, National University of Singapore, Singapore 119260

Contributed by Roscoe O. Brady, December 30, 1998

ABSTRACT **Niemann–Pick type C disease (NP-C) is an inherited neurovisceral lipid storage disorder characterized by progressive neurodegeneration. Most cases of NP-C result from inactivating mutations of *NPC1*, a recently identified member of a family of genes encoding membrane-bound proteins containing putative sterol sensing domains. By using a specific antipeptide antibody to human NPC1, we have here investigated the cellular and subcellular localization and regulation of NPC1. By light and electron microscopic immunocytochemistry of monkey brain, NPC1 was expressed predominantly in perisynaptic astrocytic glial processes. At a subcellular level, NPC1 localized to vesicles with the morphological characteristics of lysosomes and to sites near the plasma membrane. Analysis of the temporal and spatial pattern of neurodegeneration in the NP-C mouse, a spontaneous mutant model of human NP-C, by amino–cupric–silver staining, showed that the terminal fields of axons and dendrites are the earliest sites of degeneration that occur well before the appearance of a neurological phenotype. Western blots of cultured human fibroblasts and monkey brain homogenates revealed NPC1 as a 165-kDa protein. NPC1 levels in cultured fibroblasts were unchanged by incubation with low density lipoproteins or oxysterols but were increased 2- to 3-fold by the drugs progesterone and U-18666A, which block cholesterol transport out of lysosomes, and by the lysosomotropic agent NH_4Cl. These studies show that NPC1 in brain is predominantly a glial protein present in astrocytic processes closely associated with nerve terminals, the earliest site of degeneration in NP-C. Given the vesicular localization of NPC1 and its proposed role in mediating retroendocytic trafficking of cholesterol and other lysosomal cargo, these results suggest that disruption of NPC1-mediated vesicular trafficking in astrocytes may be linked to neuronal degeneration in NP-C.**

Niemann–Pick type C disease (NP-C) is a progressive and fatal neurodegenerative disorder that has been linked to two separate genetic loci, *NPC1* (major locus) and *NPC2* (1–3). The human *NPC1* gene has been identified recently through positional cloning and shown to encode a 1,278-aa protein, which shares homology with several proteins that regulate cholesterol homeostasis such as 3-hydroxy-3-methylglutaryl-CoA (HMG CoA) reductase and sterol regulatory element binding protein cleavage-activating protein (SCAP), as well as with PATCHED, the receptor for the morphogen Sonic hedgehog (4). The chromosomal location and identity of the *NPC2* gene remain unknown, although mutations in both *NPC* genes cause identical biochemical and clinical NP-C phenotypes.

The predicted structure of the NPC1 protein contains several functional domains including a unique NPC segment that is highly conserved between the human, mouse, *Caenorhabditis elegans*, and *Saccharomyces cerevisiae* NPC1 homologs, and 13 putative transmembrane domains that include a potential sterol sensing domain. The NPC domain (residues 55–164) is marked by 8 cysteine residues with conserved spacing between all *NPC1* orthologs (4, 5). Within this domain is a leucine zipper motif (residues 73–94), which may be the site of interaction with other proteins. Human NP-C is caused by insertion, deletion, and missense mutations of the *NPC1* gene (4). A spontaneous mouse model of NP-C, the BALB/c *NPC1*$^{-/-}$ mouse, which shows disruption of the *NPC1* gene, is characterized by an intronic insertion of retrotransposon-like sequences from the mammalian apparent long terminal repeat-retrotranspon (MaLR) family, which causes a frame shift and protein truncation before the sterol sensing domain (5, 6). These animals display biochemical and neurological features similar to the human disease (7).

To study the cellular and subcellular localization and regulation of NPC1, we have generated polyclonal antipeptide antibodies to human NPC1. We have shown that in cultured human fibroblasts, NPC1 is associated with a late endocytic compartment that functions in the vesicular movement of endocytosed cargo from lysosomes to other cellular sites (8). Because of the unique vulnerability of the brain in NP-C, we have here mapped the expression of NPC1 in primate brain by light and electron microscopic immunocytochemistry and correlated the findings with the developmental pattern of neurodegeneration in NP-C mouse brain by using a sensitive silver staining procedure (9). In addition, we have investigated the regulation of NPC1 protein in cultured human fibroblasts by sterols and agents that block lysosomal cholesterol transport or disrupt lysosomal pH gradients. We show that NPC1 is predominantly a glial protein present in astrocytic processes closely associated with nerve terminals, the earliest site of degeneration in NP-C. NPC1 localizes to LAMP2 positive vesicles and to sites near the plasma membrane. NPC1 levels are not modulated by changes in cellular cholesterol content but are increased by agents that block cholesterol transport out of lysosomes or which disrupt lysosomal pH (10). In addition to the proposed role of NPC1 in mediating retroendocytic distribution of cholesterol and other lysosomal cargo, these

The publication costs of this article were defrayed in part by page charge payment. This article must therefore be hereby marked "*advertisement*" in accordance with 18 U.S.C. §1734 solely to indicate this fact.

PNAS is available online at www.pnas.org.

Abbreviations: LDL, low density lipoprotein; NP-C, Niemann–Pick type C disease; HMG CoA, 3-hydroxy-3-methylglutaryl-CoA; CHO, Chinese hamster ovary.

†To whom reprint requests should be addressed at: Neurobiology Research Laboratory, VA Connecticut Healthcare System, 555 Willard Avenue, Newington, CT 06111. e-mail: patel.shutish_c@westhaven.va.gov.

results suggest that disruption of NPC1-mediated functions in astrocytes may play a role in neuronal degeneration in NP-C.

MATERIALS AND METHODS

Animals. Monkey brain tissue for Western blots was obtained from a colony of African Green monkeys at St. Kitts Biomedical Research Foundation and was provided through the courtesy of J. Elsworth and D. Redmond (Department of Psychiatry, Yale University, New Haven, CT). For immunocytochemistry, brain was obtained from adult male and female *Macaca fascicularis* monkeys maintained at the National University of Singapore.

BALB/c *NPC1*$^{-/-}$ mice were obtained from a colony maintained in our laboratory. The biochemical and phenotypic features of these mice resemble human NP-C and have been described previously (5, 7). Control animals were from a separate colony of wild-type BALB/c mice. All animal procedures were approved by the respective Institutional Animal Care and Use Committees and were in accordance with the U.S. Public Health Service guide for the care and use of laboratory animals.

Cells. Normal human fibroblasts were obtained from the American Type Culture Collection (CRL-1489) and from volunteers at the Developmental and Metabolic Neurology Branch under the guidelines approved by the National Institute of Neurological Disorders and Stroke Intramural Review Board. Human fetal astrocyte cultures were kindly provided by J. Antel (Montreal Neurological Institute, McGill University). Cultures were prepared from fetal tissue obtained by therapeutic abortion with informed consent and approval of local hospital ethics committees in accordance with guidelines provided by the Medical Research Council of Canada. Fibroblasts were also obtained from a neonate ("MP") with a rapidly progressive and fatal form of NP-C. MP was the second child with NP-C born to consanguinous parents. Northern blots of "MP" fibroblasts revealed the complete absence of *NPC1* mRNA (data not shown), indicating that she was an *NPC1* null mutant. Chinese hamster ovary (CHO) cells from the mutant cell line CT60, which display an NP-C phenotype, were generously provided by T. Y. Chang (Dartmouth University, Hanover, NH). CT60 cells transfected with yeast artificial chromosome 911D5 (designated "D5B5" cells), which contains the *NPC1* gene which has been shown to correct the NP-C phenotype, have been described (11). All cells were cultured in DMEM containing 10% fetal bovine serum and 1% penicillin/streptomycin.

Preparation of Antipeptide NPC1 Antibodies. Rabbit polyclonal antisera were raised against keyhole limpet hemocyanin conjugates of synthetic peptides derived from the predicted structure of NPC1 (4) as follows: NH2-CDVRQLQTLKDNLQLPLQF-COOH (residues 75–93), antibody NPC1-L; NH2-YVGQSFANAMYNACRDVEA-COOH (residues 147–165), antibody NPC1-N; and NH2-NKAKSCATEERYKGTERER-COOH (residues 1256–1274), antibody NPC1-C. Amino acids 75–93 span the leucine zipper domain of NPC1, residues 147–165 are part of the conserved NPC domain, and residues 1256–1274 represent the penultimate portion (excluding the terminal tetrapeptide LLNF) of the relatively short (27-aa) carboxyl tail of human NPC1. Antisera were screened by dot blot analysis using the immunizing peptide as antigen. Antibodies were then affinity purified by reacting with the immunizing peptides linked to cyanogen bromide-activated Sepharose 4B according to the manufacturer's protocol (Pharmacia). Mock affinity-purified antibodies were obtained by passage and elution of preimmune sera over the affinity columns.

Western Blots. All procedures were performed on ice, because pilot studies showed that heating to 37°C or boiling the cell or tissue lysates resulted in >90% loss of NPC1 immunoreactivity. Confluent fibroblast monolayers were lysed in a buffer containing 50 mM Tris (pH 8.0), 150 mM NaCl, 1% Nonidet P-40, 100 μg/ml phenylmethylsulfonyl fluoride (PMSF), and 1 μg/ml aprotinin. Tissue punches from cortex and subcortical white matter obtained from frozen brain tissue of four adult African Green monkeys were homogenized on ice in 0.32 M sucrose containing 100 μg/ml PMSF and 1 μg/ml aprotinin. Cell lysates and homogenates (40–50 μg) were electrophoresed through SDS/5% polyacrylamide gels under reducing conditions, transferred to nitrocellulose membranes, and Western blotted for NPC1. Of the three antipeptide antibodies, NPC1-C revealed the brightest staining by immunofluorescence and accordingly was selected for all Western blot and immunocytochemical analyses described here. Immunoreactive bands were visualized by using peroxidase-conjugated donkey anti-rabbit secondary IgG and enhanced chemiluminescence detection (Amersham). Signals were quantitated by densitometry using an LKB ultroscan XL laser densitometer (Pharmacia LKB).

Amino–Cupric–Silver Staining. To determine the spatial and temporal pattern of neurodegeneration in NP-C we performed a sensitive amino–cupric–silver staining procedure to delineate disintegrative changes (9). NP-C mice (1, 10, 20, 43, 61, and 72 days old) and a 70-day-old wild-type mouse were perfused transcardially with freshly prepared, ice-cold 4% paraformaldehyde, and the brains were removed and embedded in a 4×4 array in a gelatin matrix using MultiBrain Technology (NeuroScience Associates, Knoxville, TN). Sections (30 μM) were obtained on a sliding microtome (American Optical) and processed for amino–cupric–silver staining. Homozygous NP-C mice 40 days and older were identified by their characteristic neurological phenotype, and the homozygous status of all animals (neonatal and adult mice) was confirmed by their reduced hepatic lysosomal sphingomyelinase activities as described (12).

Immunocytochemistry. Four adult male and female *M. fascicularis* monkey brains were processed for NPC1 immunocytochemistry. The animals were deeply anesthetised with Nembutal (30 mg/kg i.p.), perfused transcardially with normal saline, and perfusion-fixed with 4% paraformaldehyde/0.1% glutaraldehyde in 0.1 M phosphate buffer (pH 7.4). The brains were removed and blocks of frontal and temporal neocortex were dissected and post-fixed in the same fixative overnight. Sections (100 μM) were processed for immunocytochemistry by using either horseradish peroxidase or immunogold detection systems. For peroxidase immunocytochemistry, sections were washed for 3 hr in PBS to remove traces of fixative and incubated for 1 hr in 5% normal goat serum (NGS) in PBS to block nonspecific antibody binding. Sections were then incubated overnight with NPC1-C antiserum (diluted 1:500 in PBS), washed three times in PBS, incubated for 1 hr at room temperature in a 1:200 dilution of biotinylated goat anti-rabbit IgG (Vector Laboratories), and processed for light and electron microscopic peroxidase immunocytochemistry (13, 14). For immunogold labeling, sections were incubated overnight with NPC1-C antiserum (diluted 1:250 in buffer A: 1% NGS/0.1% Tween 20/1% BSA/0.1% sodium azide in PBS, pH 8.2), washed for 1 hr in buffer A, and incubated for 3 hr at room temperature with goat anti-rabbit IgG conjugated to 1 nM gold particles (diluted 1:100, British BioCell International, Cardiff, U.K.). After successive 30-min washes in buffer A and PBS to remove excess gold conjugate, sections were fixed in 1% glutaraldehyde for 10 min, washed in distilled water for 30 min, and then immersed in fresh silver enhancing solution (British BioCell International) for 20–25 min and washed thoroughly in distilled water. Some of the sections were mounted on gelatinized slides, dehydrated, and coverslipped, whereas others were processed further for electron microscopy.

Electron Microscopy. Electron microscopy was carried out by dissecting the immunoperoxidase and immunogold labeled sections into smaller rectangular portions that included the entire thickness of the cerebral cortex. Sections were osmicated, dehydrated in an ascending series of ethanol and acetone, and embedded in Araldite. Thin sections were obtained from the first 5 μm of the immunostained sections mounted on copper grids coated with Formvar and stained with uranyl acetate and lead citrate. They were viewed by using a Philips CM120 Biotwin or Jeol 1200EX electron microscope.

Confocal Microscopy. Human fetal astrocytes were grown on glass coverslips, fixed in 4% paraformaldehyde, and processed for double-label fluorescence colocalization of NPC1 and LAMP2 (a marker for late endosomes and lysosomes) (8, 15) by using NPC1-C primary antibody (1:400) with rhodamine-conjugated anti-rabbit IgG secondary antibody (1:100) or mouse monoclonal anti-human LAMP2 IgG primary antibody (1:250) and fluorescein-conjugated goat anti-mouse IgG (1:100) (8, 13, 16). The fluorescent images were visualized on a Zeiss LSM410 confocal microscope equipped with an Argon/Krypton laser.

Control sections for all immunocytochemistry of NPC1 were incubated with mock affinity-purified preimmune rabbit serum or with NPC1-C antibody absorbed with immunizing peptide (2 μg/μl).

RESULTS

Specificity of Anti-NPC1 Antibody. Western blots of normal human fibroblasts and monkey brain homogenates revealed NPC1 as a broad immunoreactive band of molecular mass =165 kDa (Figs. 1 and 2). A slightly higher sized band was observed in D5B5 cells probably because of differential posttranslational processing of NPC1 protein in CHO cells transfected with yeast artificial chromosome 911D5. As expected, NPC1 protein was absent in Western blots of MP fibroblasts and CT60 cells. In addition, it was not detected when the primary antibody was replaced with mock affinity-purified preimmune serum (not shown) or antigen absorbed antibody. These findings thus validate the 165-kDa immunoreactive band as the NPC1 protein.

Expression of NPC1 in Monkey Brain. Peroxidase immunocytochemistry of monkey brain cortex revealed immunoreactivity confined mainly to cell processes in the neuropil (Fig. 3 *B* and *C*). Cell bodies were either unlabeled or weakly labeled. The immunoreactivity observed with NPC1-C antibody was specific and was eliminated in sections incubated with preimmune serum or with antigen-absorbed antibody (Fig. 3*A*). By electron microscopy, NPC1 immunoreactivity was localized in astrocytic processes (Fig. 3 *D* and *E*), near the cell membrane of the soma (Figs. 3*E* and 4*B*), and in lysosomes (Fig. 4 *A–C*), but was absent from the nucleus and perinuclear cytoplasm. The absence of staining over the central portions of the soma likely accounts for the indistinct staining of the astrocytic cell bodies by light microscopy. NPC1 labeled processes had irregular outlines, were often present on one side of asymmetrical synapses between unlabeled axon terminals and dendrites, and could be traced to their parent

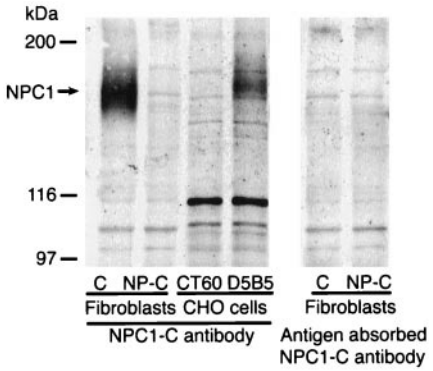

FIG. 1. Western blot analysis with NPC1-C antibody of normal human fibroblasts (C), fibroblasts from an NP-C patient (NP-C), CHO cells from the mutant cell line CT60 that display an NP-C phenotype (CT60), and CT60 cells transfected with yeast artificial chromosome 911D5 containing the *NPC1* gene (D5B5). Normal fibroblasts express NPC1 as a 165 kDa protein that is absent in NP-C fibroblasts and in CT60 CHO cells. A slightly larger sized NPC1 band is observed in D5B5 cells probably because of differential posttranslational processing of NPC1 in CHO cells. The NPC1 immunoreactive band is completely abolished by preincubation with antibody absorbed with NPC1-C peptide. Representative of three separate experiments.

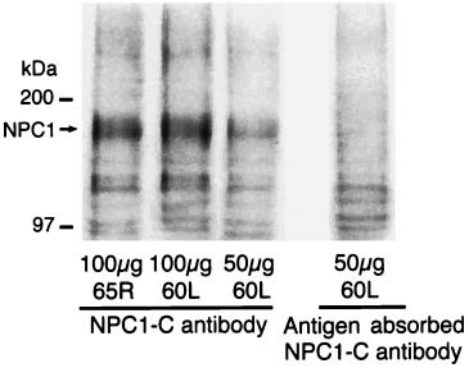

FIG. 2. Western blots of monkey brain homogenates of right dorsolateral frontal (65R) and left orbital frontal (60L) cortex. NPC1 is detected as a 165-kDa immunoreactive band that is completely abolished by preincubation of NPC1-C antibody with immunizing peptide.

astrocytic cell bodies (Fig. 3*E*). These characteristics were identical to those reported for glutamine synthetase positive astrocytic processes (14). Neuronal cell bodies and processes including axon terminals, small diameter dendrites postsynaptic to axon terminals, and larger diameter dendritic shafts containing parallel arrays of microtubules were unlabeled. Other types of glial cells with dense heterochromatin clumps in the nucleus and features of oligodendrocytes or microglia, as well as mural cells in the walls of blood vessels, were also unlabeled. Staining was also completely absent in the subcortical white matter.

Confocal Microscopy. By confocal microscopy (Fig. 5), rhodamine-labeled NPC1 immunoreactivity (red) was localized predominantly in cytoplasmic vesicles in a perinuclear distribution. Simultaneous fluorescein localization of LAMP2 (green) revealed immunoreactivity in cytoplasmic vesicles distributed in both a perinuclear and peripheral pattern (Fig. 5 *Middle*). Overlapping of the NPC1 and LAMP2 immunoreactive images (yellow) revealed NPC1 in a subset of perinuclear LAMP2 positive vesicles (Fig. 5 *Bottom*).

Neurodegenerative Changes in NP-C Mouse Brain. To characterize the temporal and spatial pattern of neurodegeneration in NP-C mice, whole brains of control and affected mice were characterized neuropathologically by using an amino–cupric–silver stain to delineate disintegrative changes (Fig. 6) (9). In contrast to normal mice that showed a complete absence of silver labeled structures in the cortex (Fig. 6*A*), NP-C mice showed degeneration within the neuropil of the cortex and in white matter tracts including the corpus callosum in animals as early as 22 days of age (Fig. 6*B*). The amount of degeneration increased with age, and in sections of older mice densely stained cell bodies were observed in the cortex in addition to the dense staining of the neuropil (Fig. 6*C*). Because NP-C mice do not display neurological symptoms until about 40 days of age, these findings suggest that there must be considerable cumulative neurodegeneration before phenotypic signs are manifest. Marked degeneration was also observed in the neuropil in the hippocampus although very few degenerating cell bodies were observed in the strata pyramidale and granulosum (Fig. 6*C*).

Modulation of NPC1 in Cultured Fibroblasts. NPC1 has a putative membrane-associated sterol-sensing domain similar to that of HMG CoA reductase, whose activity is known to be modulated by changes in cellular cholesterol content. For instance, in cultured cells, HMG CoA reductase is rapidly degraded when cellular sterol levels rise and its synthesis is suppressed by oxysterols such as 25-hydroxycholesterol and 7-ketocholesterol (17). To assess whether NPC1 is regulated by sterols, we determined changes in NPC1 protein levels in cultured fibroblasts incubated with LDL or oxysterols. As shown in Table 1, there was no significant change in NPC1 content in fibroblasts incubated with either of these two agents indicating that NPC1 is not

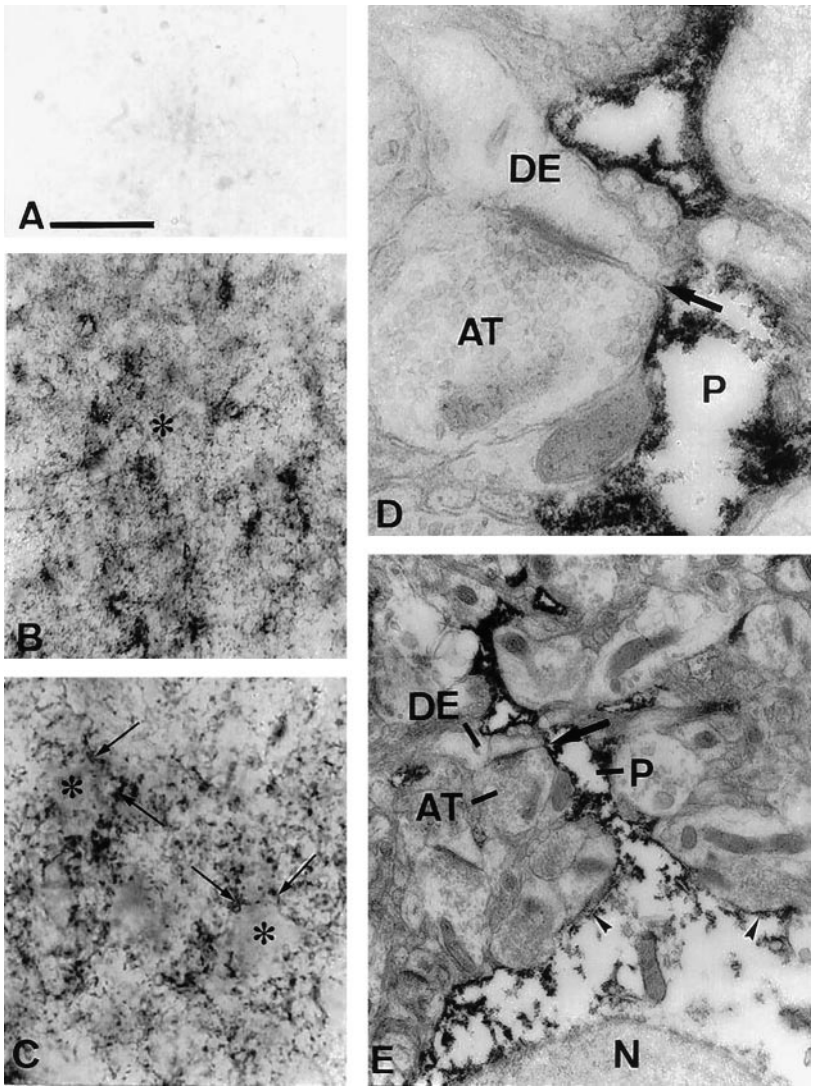

FIG. 3. Expression of NPC1 in monkey temporal cortex by light (*A–C*) and electron microscopic (*D* and *E*) peroxidase immunocytochemistry. (*A*) Control section incubated with antigen-absorbed NPC1-C antibody showing complete absence of staining. (*B*) Layer three of cortex showing NPC1 immunoreactivity localized predominantly in processes in the neuropil (*). (*C*) Higher magnification of layer three showing unlabeled cell bodies (*) surrounded by large numbers of NPC1 positive processes (arrows). (*D*) Astrocytic process (P) in the neuropil. These processes are present at the sides of asymmetrical synapses (arrows in *D* and *E*) between unlabeled axon terminals (AT) and dendrites (DE). (*E*) Same process (P) as in *D*, on the side of an asymmetrical synapse (arrow) between an unlabeled axon terminal (AT) and dendrite (DE). The process can be traced to its parent cell body. Label is present in the process and near the cell membrane of the soma (arrowheads), but is absent from the nucleus (N) and more central regions of the cytoplasm. [Bars = 16 μm (*A* and *C*), 80 μm (*B*), 0.3 μm (*D*), and 1 μm (*E*).]

modulated by changes in overall cellular cholesterol content. In contrast, incubation of fibroblasts with drugs that are known to block the transport of cholesterol out of lysosomes, e.g., progesterone or the amphipathic amine U-18666A, or with the lysosomotropic agent NH_4Cl, resulted in a 2- to 3-fold increase in NPC1 protein (Table 1).

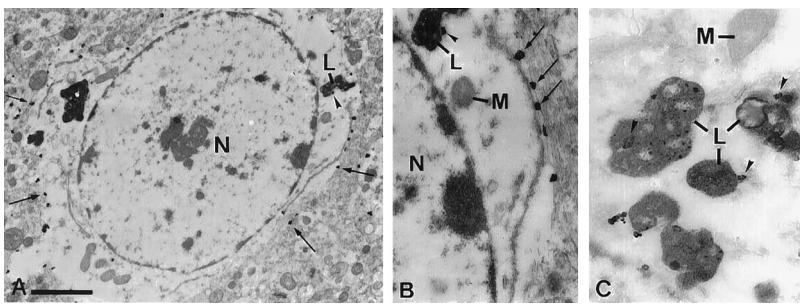

FIG. 4. Electron micrographs showing the distribution of NPC1 immunoreactivity by immunogold/silver labeling in monkey frontal cortex. (*A*) Cell body of an astrocyte showing gold/silver complexes at the periphery of the cell (arrows) and in association with a lysosome (L, arrowhead). Label is absent from the nucleus (N) and the perinuclear cytoplasm. (*B*) Higher magnification of *A* showing a punctate pattern of gold/silver complexes near the cell membrane (arrows) and on the lysosome (L, arrowhead). The nucleus (N) and mitochondria (M) are unlabeled. (*C*) Gold-labeled lysosomes (L, arrowheads) and unlabeled mitochondrion (M) from another astrocyte. [Bars = 1.8 μm (*A*) and 0.7 μm (*B* and *C*).]

DISCUSSION

In this study, we have mapped the expression of NPC1 in brain by light and electron microscopic immunocytochemistry and shown that it is predominantly a glial protein present in astrocytic processes closely associated with synapses. We demonstrate that neurodegeneration in NP-C brain is established well before the appearance of neurological symptoms and that terminal axonal and dendritic fields, which are closely associated with NPC1-containing perisynaptic astrocytic processes, are the earliest structures to degenerate.

In cultured human astrocytes we found NPC1 in the cores of LAMP2 containing cytoplasmic vesicles. A similar vesicular localization of NPC1 has also been found in fibroblasts in which NPC1 is a component of a subset of cholesterol-free late endosomes that interact transiently with LDL-derived cholesterol-enriched lysosomes (8). By kinetic analysis of the clearance of endocytosed [^{14}C]sucrose, NPC1 was shown to function in the retroendocytic transport of lysosomal cargo including cholesterol (8). Localization of NPC1 to the cores of LAMP2 positive vesicles appears to be obligatory for its cholesterol mobilizing function because mutation of the conserved cysteine residues in the NPC domain results in a protein that fails to localize to the central core of cholesterol-laden lysosomes in CT60 cells and deletion of the

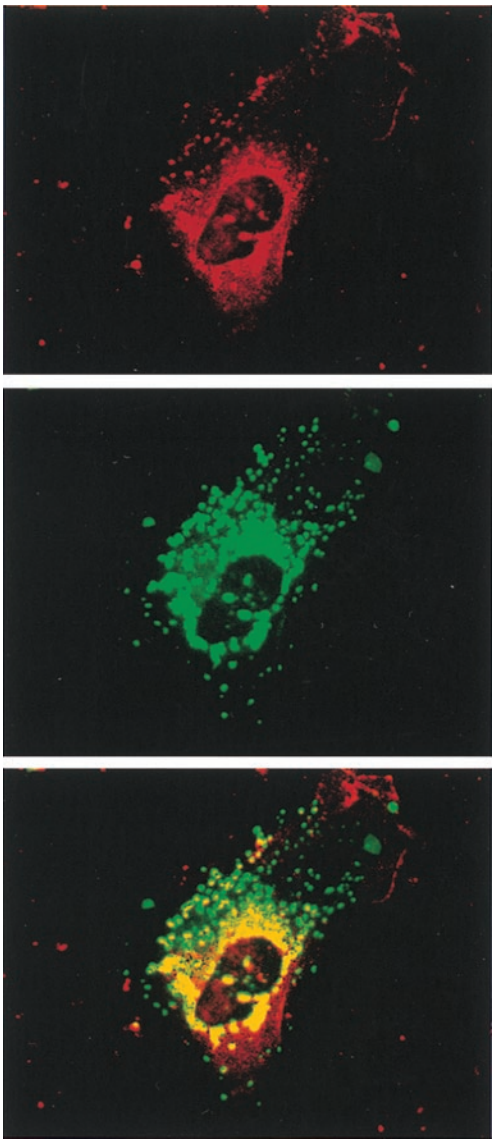

FIG. 5. Confocal microscopic images of cultured human astrocytes showing localization of NPC1 by rhodamine fluorescence (red), LAMP2 by fluorescein fluorescence (green), and colocalization of the two antigens (yellow/orange). NPC1 is present in perinuclear cytoplasmic vesicles. LAMP2 localizes to cytoplasmic vesicles distributed around the nucleus as well as in the periphery of the cell (*Middle*). Overlapping the images reveals colocalization of NPC1 within the cores of LAMP2 positive vesicles (*Bottom*).

Table 1. Regulation of NPC1 protein by sterols and lysosomotropic agents in cultured human fibroblasts

Culture conditions	NPC1
LPDS	100
LDL	114
25-hydroxycholesterol	110
7-keto cholesterol	111
U-18666A	215
Progesterone	244
NH_4Cl	270

Normal human fibroblasts were grown to confluency in Eagle's MEM supplemented with 10% FBS, followed by incubation for 3 days in McCoy's medium containing 5% LDL-deficient serum (LPDS) (medium A). Cells were trypsinized and seeded in medium A for an additional 3 days with or without LDL (10 μg/ml), 25-hydroxycholesterol (2 μg/ml), 7-keto cholesterol (2 μg/ml), progesterone (10 μg/ml), the amphipathic amine U-18666A (2 μg/ml), or NH_4Cl (10 mM). Cell extracts were analyzed by western blots for NPC1 and immunoreacive bands quantitated by densitometry. Results are expressed relative to LPDS taken as 100%. Representative of three separate analyses.

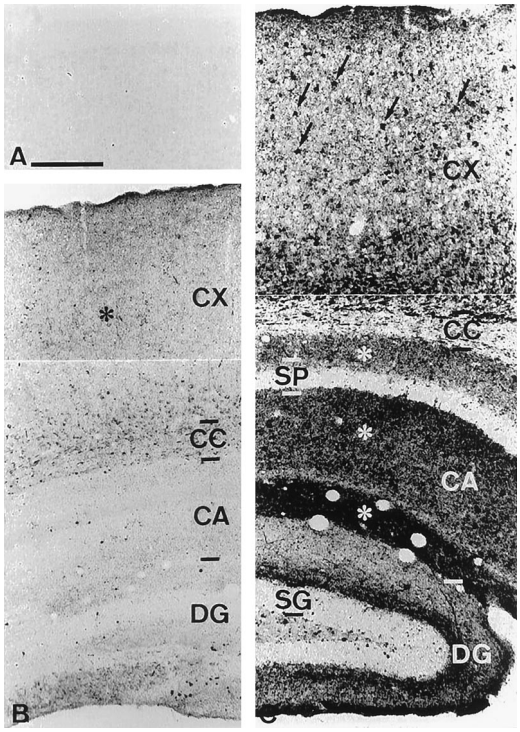

FIG. 6. Neurodegeneration in NP-C mouse brain revealed by amino–cupric–silver staining. (*A*) Layers I–III of the cortex of a 22-day-old normal mouse showing absence of degenerating structures. (*B*) Section through the temporal neocortex (CX), corpus callosum (CC), cornu ammonis field CA1 (CA), and dentate gyrus (DG) of a 22-day-old NP-C mouse. Many degenerating terminals are present in the neuropil of the cerebral cortex (*), although there are few labeled cell bodies (c.f., *C*). (*C*) Section through the temporal neocortex, corpus callosum (CC), cornu ammonis field CA1 (CA), and dentate gyrus (DG) of a 72-day-old NP-C mouse. Large numbers of labeled cell bodies are present in the cerebral cortex (arrows) in addition to the degenerating terminals. Marked degeneration is also observed in the neuropil of the hippocampus, although few degenerating cell bodies are observed in the strata pyramidale (SP) and granulosum (SG). [Bars = 250 μm (*A* and *B*) and 330 μm (*C*).]

C-terminal tetrapeptide (LLNF) causes NPC1 to remain in the endoplasmic reticulum (18). Both *NPC1* mutations resulted in mutant NPC1 proteins that failed to mobilize lysosomal cholesterol in CT60 cells. Given such a role for NPC1 in vesicular trafficking, our finding of its localization in perisynaptic astrocytic processes raises the possibility that defective vesicular transport of cholesterol may be an important factor leading to the neurodegeneration in NPC. A trafficking pathway for delivery of nutrients and metabolites between astrocytes and neurons is supported by previous studies. Astrocytes have been implicated in the delivery of glucose and lactate to neurons (19) and are known to play an important role in the uptake and recycling of neuronally released glutamate (20). In this respect it is of interest that glutamine synthetase in human cerebral cortical astrocytes is localized in a manner that closely resembles the perisynaptic astrocytic localization of NPC1 in this study (16).

NPC1 belongs to the family of membrane bound proteins, which include HMG CoA reductase, SCAP, and PATCHED, that share sequence similarity in their transmembrane domains (4). The conserved transmembrane domains in these proteins have been implicated as putative sterol sensors because the presence of such a domain is both necessary and sufficient for the sterol-mediated degradation of HMG CoA reductase (21, 22). We found that fluctuations in cellular cholesterol do not alter NPC1 levels. Thus, the putative sterol-sensing domains of NPC1 may be responsive to changes in vesicular membrane cholesterol and modulate vesicular function as has been suggested previously (8). Agents that block cholesterol transport out of lysosomes or that disrupt lysosomal pH increase its concentration 2- to 3-fold. Because progesterone traps NPC1 in cholesterol-laden lysosomes (8), it is possible that the increased accumulation of cellular NPC1 protein induced by such drugs is due to abnormal sequestration and/or reduced turnover of the protein in lysosomes.

There are a number of distinctive features of cholesterol metabolism in brain compared with peripheral tissues. In the brain and spinal cord, cholesterol is synthesized almost exclusively *in situ* with very slow turnover and little contribution from the plasma (23–26). By differential analysis of lipid synthesis in neuronal somata and axon terminals of cultured rat sympathetic neurons, Vance *et al.* (27) found that axons have the capacity to synthesize phospholipids and sphingomyelin, but not cholesterol. This suggests that neuronal processes may have a requirement for cholesterol delivery from exogenous sources such as astrocytes. In this respect, it is of interest that several apolipoproteins that mediate cholesterol transfer functions in plasma, as well as lipoprotein receptors such as the LDL receptor (LDLR) and LDLR-related protein (LRP), are also expressed in neural tissues (28–30). Functional disruption of the LDLR and apoE genes in mice, however, do not cause gross neurological abnormalities (31, 32), and neither apoE nor apoA1 within lipoproteins are essential for axonal growth *in vitro* (33). On the other hand, apoD, a cholesterol binding protein that is synthesized in large amounts by regenerating nerves, is induced more than 30-fold in NP-C mouse brain (34–36). Both apoD and apoE are normally secreted constitutively from cultured astrocytes, whereas secretion of apoD (but not apoE) from NP-C astrocytes is markedly reduced (37). In addition, apoD, but not apoE, secretion from normal astrocytes is differentially stimulated by the oxysterol 25-hydroxycholesterol, suggesting that this process is sterol dependent. Taken together with our current observation of the astrocytic localization of NPC1 and its role in vesicular trafficking (8), neuronal degeneration in NP-C may be linked to deficient NPC1 and apoD-mediated lipid transport in neural cells.

NPC1 appears to play a role in vesicular trafficking in glia, a process that may be crucial for maintaining the structural and functional integrity of nerve terminals. This notion is supported by the findings that (*i*) NPC1 is expressed in perisynaptic processes of astrocytes and (*ii*) mutations of NPC1 result in degeneration of terminal fields of axons and dendrites before degeneration of neuronal cell bodies. Further studies designed to correlate the spatial and temporal pattern of neurodegeneration and lipid storage in NP-C with NPC1 expression could provide insights into the role of NPC1 in lipid trafficking in the brain.

This paper is dedicated to the memory of Michael Deselm. We thank Dr. T. Y. Chang for the gift of CT60 cells, Geetha Suresh and Adnan Butt for expert technical assistance, and Elizabeth Palm for assistance with manuscript preparation. This work was supported by National Institutes of Health Grants NS34339 (S.C.P.) and NS32160 (Y.C.P.).

1. Pentchev, P. G., Vanier, M. T., Suzuki, K. & Patterson, M. C. (1995) in *The Metabolic and Molecular Basis of Inherited Diseases*, eds. Scriver, C. R., Beaudet, A. L., Sly, W. S., Valle, D. D. (McGraw-Hill, New York), pp. 2625–2639.
2. Patel, S. C., Barton, N. W. & Argoff, C. (1992) in *Handbook of Clinical Neurology*, ed. de Jong, J. M. B. V. (Elsevier Science, Rotterdam, The Netherlands), Vol. 16, pp. 147–164.
3. Vanier, M. T., Duthel, S., Rodriguez-Lafrasse, C., Pentchev, P. & Carstea, E. D. (1996) *Am. J. Hum. Genet.* **58,** 118–125.
4. Carstea, E. D., Morris, J. A., Coleman, K. G., Loftus, S. K., Zhang, D., Cummings, C., Gu, J., Rosenfeld, M. A., Pavan, W. J., Krizman, D. B., *et al.* (1997) *Science* **277,** 228–231.
5. Loftus, S. K., Morris, J. A., Carstea, E. D., Gu, J. Z., Cummings, C., Brown, A., Ellison, J., Ohno, K., Rosenfeld, M. A., Tagle, D. A., *et al.* (1997) *Science* **277,** 232–235.
6. Pentchev, P. G., Gal, A. E., Booth, A. D., Omodeo-Sale, F., Fouks, J., Neumeyer, B. A., Quirk, J. M., Dawson, G. & Brady, R. O. (1980) *Biochim. Biophys. Acta* **619,** 669–679.
7. Patel, S. C. & Pentchev, P. G. (1989) *Annu. Rev. Nutr.* **9,** 395–416.
8. Neufeld, E. B., Wastney, M., Patel, S., Suresh, S., Cooney, A. M., Dwyer, N. K., Roff, C. F., Ohno, K., Morris, J., Carstea, E. D., *et al.* (1999) *J. Biol. Chem.,* in press.
9. de Olmos, J. S., Beltramino, C. A. & de Olmos de Lorenzo, S. (1994) *Neurotoxicol. Teratol.* **16,** 545–561.
10. Butler, J. D., Blanchette-Mackie, J., Goldin, E., O'Neill, R. R., Carstea, G., Roff, C. F., Patterson, M. C., Patel, S. C., Comly, M. E., Cooney, A., *et al.* (1992) *J. Biol. Chem.* **267,** 23797–23805.
11. Gu, J. Z., Carstea, E. D., Cummings, C., Morris, J. A., Loftus, S. K., Zhang, D., Coleman, K. G., Cooney, A. M., Comly, M. E., Fandino, L., *et al.* (1997) *Proc. Natl. Acad. Sci. USA* **94,** 7378–7383.
12. Patel, S. C., Suresh, S., Weintroub, H., Brady, R. O. & Pentchev, P. G. (1987) *Biochem. Biophys. Res. Commun.* **143,** 233–240.
13. Kumar, U., Asotra, K., Patel, S. C. & Patel, Y. C. (1997) *Exp. Neurol.* **145,** 412–424.
14. Ong, W. Y., Garey, L. J. & Reynolds, R. (1993) *J. Neurocytol.* **22,** 893–902.
15. Chen, J. W., Murphy, T. L., Willingham, M. C., Pastan, I. & August, J. T. (1985) *J. Cell Biol.* **101,** 85–95.
16. Kumar, U. K., Sasi, S., Suresh, S., Patel, A., Thangaraju, M., Metrakos, P., Patel, S. C. & Patel, Y. C. (1999) *Diabetes* **48,** 77–85.
17. Gil, G., Faust, J. R., Chin, D. J., Goldstein, J. L. & Brown, M. S. (1985) *Cell* **41,** 249–258.
18. Skalnik, D. G., Narita, H., Kent, C. & Simoni, R. D. (1988) *J. Biol. Chem.* **263,** 6836–6841.
19. Watari, H., Blanchette-Mackie, E. J., Dwyer, N. K., Glick, J., Patel, S., Neufeld, E. B., Brady, R. O., Pentchev, P. G. & Strauss, J. F., III (1999) *Proc. Natl. Acad. Sci. USA* **96,** 805–810.
20. Forsyth, R., Fray, A., Boutelle, M., Fillenz, M., Middleditch, C. & Burchell, A. (1996) *Dev. Neurosci.* **18,** 360–370.
21. Faust, J. R., Luskey, K. L., Chin, D. J., Goldstein, J. L. & Brown, M. S. (1982) *Proc. Natl. Acad. Sci. USA* **79,** 5205–5209.
22. Westergaard, N., Sonnewald, U. & Schousboe, A. (1995) *Dev. Neurosci.* **17,** 203–211.
23. Jurevics, H. & Morell, P. (1995) *J. Neurochem.* **64,** 895–901.
24. Turley, S. D., Burns, D. K., Rosenfeld, C. R. & Dietschy, J. M. (1996) *J. Lipid Res.* **37,** 1953–1961.
25. Turley, S. D., Burns, D. K. & Dietschy, J. M. (1998) *Am. J. Physiol.* **274,** E1099–E1105.
26. Wilson, J. D. (1970) *J. Clin. Invest.* **49,** 655–665.
27. Vance J. E., Pan, D., Campenot, R. B., Bussiere, M. & Vance, D. E. (1994) *J. Neurochem.* **62,** 329–337.
28. Pitas, R. E., Boyles, J. K., Lee, S. H., Hui, D. & Weisgraber, K. H. (1987) *J. Biol. Chem.* **262,** 14352–14360.
29. Swanson, L. W., Simmons, D. M., Hofmann, S. L., Goldstein, J. L. & Brown, M. S. (1988) *Proc. Natl. Acad. Sci. USA* **85,** 9821–9825.
30. Herz, J., Hamann, U., Rogne, S., Mykelbost, O., Gausepohl, H. & Stanley, K. K. (1988) *EMBO J.* **7,** 4119–4127.
31. Zhang, S. H., Reddick, R. L., Piedrahita, J. A. & Maeda, N. (1992) *Science* **258,** 468–471.
32. Ishibashi, S., Brown, M. S., Goldstein, J. L., Gerard, R. D., Hammer, R. E. & Herz, J. (1993) *J. Clin. Invest.* **92,** 883–893.
33. de Chaves, E. I., Rusinol, A. E., Vance, D. E., Campenot, R. B. & Vance, J. E. (1997) *J. Biol. Chem.* **272,** 30766–30773.
34. Boyles, J. K., Notterpek, L. M. & Anderson, L. J. (1990) *J. Biol. Chem.* **265,** 17805–17815.
35. Patel, R. C., Lange, D., McConathy, W. J., Patel, Y. C. & Patel, S. C. (1997) *Protein Eng.* **10,** 101–105.
36. Suresh, S., Yan, Z., Patel, R. C., Patel, Y. C. & Patel, S. C. (1998) *J. Neurochem.* **70,** 242–251.
37. Patel, S. C., Asotra, K., Patel, Y. C., McConathy, W., Patel, W. J., Patel, R. C. & Suresh, S. (1995) *NeuroReport* **6,** 653–657.